Volume 85, August 2014

ISSN 0010-938X

ELSEVIER

CORROSION SCIENCE

The Journal on Environmental Degradation of Materials and its Control

Editor-in-Chief: G. T. BURSTEIN, University of Cambridge, U.K.

An Official Journal of the Institute of Corrosion

CONTENTS

Contents continued on outside back cover

http://www.elsevier.com/locate/corsci

Corrosion Science 85 (2014) 222–231

Contents lists available at ScienceDirect

Corrosion Science

journal homepage: www.elsevier.com/locate/corsci

Investigation on the effect of nitrate ion on the critical pitting temperature of 2205 duplex stainless steel along a mechanistic approach using pencil electrode

M. Zakeri, M.H. Moayed *

Metallurgical and Material Engineering Department, Faculty of Engineering, Ferdowsi University of Mashhad, Mashhad 91775-1111, Iran

ARTICLE INFO

Article history:
Received 19 September 2013
Accepted 17 April 2014
Available online 24 April 2014

Keywords:
A. Stainless steel
B. Polarisation
B. Potentiostatic
C. Pitting corrosion

ABSTRACT

Investigation on influence of the nitrate ion on critical pitting temperature (CPT) of DSS 2205 in 0.6 M NaCl media is the aim of this research. Results revealed that 0.01 M NO_3^- has negligible effect on CPT, while 0.1 M NO_3^- causes CPT to shift to a value more than 85 °C. Then, a mechanistic approach using pencil electrode was sought based on proposed theory defining CPT as a temperature at which critical current density necessary for passivity (i_{crit}) equals to limiting current density (i_{lim}). Results indicate that nitrate ion increases CPT by increment in i_{lim} and slight decrement in i_{crit}.

1. Introduction

Encompassing both ferrite and austenite phases in almost equal quantity, makes duplex stainless steels (DSSs) as a common alloy in oil, marine and other industries which emphasise on both strength and resistance to localised corrosion [1,2]. Pitting corrosion is a kind of localised corrosion, which takes place in consequence of local breakdown of passive film in aggressive ions containing solution [3]. It is believed that pitting corrosion takes place in three distinct stages; nucleation, metastable and stable growth [4]. Alongside of study on the effect of many factors on the pitting corrosion, accomplished studies on the effect of temperature on pitting corrosion leads to introducing critical pitting temperature (CPT) as a temperature below which there is no stable pits regardless of potential [5,6]. The application of stainless steels in industries involved with higher temperatures, made researchers to study the effect of different features, like heat treatment and microstructural changes [7–10], surface roughness [11] and alloy composition [12–14] on the alloy CPT. Additionally, alongside of these studies, investigation on the effect of inorganic inhibitors such as SO_4^{2-} [15–17], MoO_4^{2-} [18,19], CrO_4^{2-} [20–22], $Cr_2O_7^{2-}$ [23] and NO_2^- [24–26] was taken in the consideration. Nitrate ion (NO_3^-) is also an inhibitor that its effect on CPT has been studied extensively. Schwenk [27] and Uhlig and Gilman [28] have indicated the inhibition effect of nitrate ion on corrosion of Fe–Cr–Ni alloys. The latter have established that due to addition of 3 wt.% of nitrate ion, pitting corrosion or sensible weight loss is prevented in 10 wt.% $FeCl_3$ [28]. Subsequent studies have stated that the critical nitrate ion concentration essential to show inhibiting effect is a proportion of Cl^- ion [29]. Chou et al. [30] studied the effect of nitrate ion on CPT of a high entropy alloy and concluded that CPT is increased 10 °C and 20 °C in the presence of 0.1 and 1 M of this ion, respectively. By using scanning electron microscopy (SEM), they also comprehended that although the presence of nitrate ion improves nucleation of pits but impedes growth of foretime pits.

Different models have been introduced to explain how nitrate ion increases the CPT. According to one theory, the competitive adsorption between Cl^- and NO_3^- ions as a result of similar mobility number of these ions [30,31], takes the basic roll in inhibition effect of nitrate ion [32]. In other words, the adsorption of chloride ions on passive layer would be affected by nitrate addition and its concentration increasing in pit solution would be prevented. Some models have related higher CPT of alloys in nitrate containing solutions to the localised reduction of nitrate ions that leads to consume acids and prevent localised acidity of the pit solution [33,34]. In other words, by nitrate addition, low pH condition necessary for pit attainment will be vanished and consequently pit growth will be retarded. As a result, temperature must be increased to reach pit stability criterion. Consequently, the CPT increases. In addition, Newman [33,34] advocated the idea that nitrate ion has no inhibition effect but on salt covered surfaces and above a critical potential associated to proportion of nitrate

* Corresponding author. Tel./fax: +98 511 8763305.
E-mail address: mhmoayd@um.ac.ir (M.H. Moayed).

http://dx.doi.org/10.1016/j.corsci.2014.04.021
0010-938X/

to Cl^- concentration with a reverse relationship. This idea was came up during studies conducted using stainless steels micro (pencil) electrode. Since this type of electrode provides a small area of alloy exposing to the environment, thus prevents formation of multiple outspread pits and helps researchers to make better understanding of single pit growth kinetic.

Based on thermodynamic calculations of pitting, Beck and Alkire [35] concluded that due to high current density in the early stages of pit growth, a salt layer inevitably precipitates at bottom of the pit. Isaacs proved that thickness of this layer controls its resistance [36]. Afterward, Isaacs and Newman [37] who employed pencil electrodes to investigate the stainless steels behaviour, suggested that at high anodic potentials, the pit dissolution is under salt layer diffusion controlled and decreasing the potential causes salt layer to dissolve. The importance of salt layer was confirmed when Frankel et al. [38] showed that the transition of metastable to stable pitting occurs in the presence of salt layer. Several researchers have investigated the precipitated salt composition in Ni alloys and steels [39–42]. Using X-ray, Isaacs et al. [39] studied the composition of precipitated salt layer in Fe–18Cr–13Ni in chloride containing solution, and suggested that salt layer is a Fe rich chloride salt containing the small amount of Cr and Ni. Further studies confirmed their observation and showed that molybdenum takes no role in the composition of salt layer precipitated in pits formed on Mo-containing stainless steel [40]. Rayment et al. [41] studied the salt precipitated in iron and 316L stainless steels and found that $FeCl_2{\cdot}4H_2O$ is the predominant composition of salt precipitated at the bottom of pits formed on both iron and 316L with difference in salt grain size. Proposing a new method of CPT identification, Salinas bravo and Newman [43] introduced CPT as a temperature at which $i_{lim} = i_{crit}$, where i_{lim} is the diffusion limiting current density as a result of salt precipitation and i_{crit} is the critical current density crucial for passivity in pit solution. After this new definition, pencil electrodes were used for investigating the effect of pit solution on CPT [17,44,45]. The formula proposed by Beck and Alkire [35] is used for calculating the diffusion controlled current density (Eq. (1)).

$$i_{lim} = \frac{nFDC_S}{\delta} \tag{1}$$

where i_{lim} represents the dissolution limiting current density, F is Faraday's constant, D is diffusion coefficient, C_S is the cation saturation concentration essential for metal salt to precipitate and δ is pit depth.

Moayed and Newman [17] by using 302 SS pencil electrode and Ernst and Newman [44] employing 304 SS foil in sulphate containing solution reported that the value of $D.C_S$ increases due to addition of sulphate ion to chloride solution. By comparing the obtained values of $D.C_S$ with ones related to solution free sulphate ion, Moayed related the increasing of pitting potential above CPT to change in $D.C_S$ value. Ernst, confirmed this result, and additionally related the shift in $D.C_S$ value to changes in the chemical composition of salt precipitated at the bottom of the pit. According to what Pistorius and Burstein have reported [46], he concluded that the salt composition changes from $FeCl_2$ to $FeCl_2 + FeSO_4$.

The effect of critical current density for passivity on CPT has been rarely studied. It is known that pit solution characteristics are literally different from bulk solution. As reported by Mankowski and Szklarska-Smialowska [47], the pH within the pit is close to zero and chloride concentration of pit solution reached to 2 N. Suzuki et al. [48] similarly reported that in a 0.5 N NaCl solution at 70 °C, the chloride ion concentration is in the range of 3.78–6.47 N and pH range is between −0.13 and 0.8 in pit solution. Newman and Shahrabi [34] investigated the effect of both alloying nitrogen and nitrate ion on the active dissolution of a high purity stainless steel in HCl medium with different chloride ion concentration. They demonstrated the positive effect of 0.3 M nitrate ion presence on anodic behaviour of low nitrogen alloy. They suggested that this positive effect could be attributed to electroreduction of this ion, which leads to acid consumption and pH increment inside the salt film. In addition, they suggested that active dissolution of low nitrogen stainless steel in 4 M HCl solution is affected by presence of 2 M NO_3^- ion similar to that happens when 0.22 wt.% nitrogen presences as an alloying element in 316L stainless steel exposed to HCl solution over a range of 3–4 M. They stated that the nitrogen alloying effect is related to surface enrichment of nitrogen that results in blocking the active dissolution of the incipient pit. Additionally, they found similar positive effect of 2 M nitrate ion to nitrogen producing is due to electroreduction of nitrate ion. But later, Misawa and Tanabe [49] using in situ Raman spectroscopy observed that the combination of oxygen existed in passive layer and alloying nitrogen leads to generation of nitrate ion on the nitrogen alloyed stainless steel surface. They suggested that the nitrate ion presented on alloy surface, improves self-healing of passive layer and consequently increases the stainless steel resistance to pitting corrosion.

In the present study, we first studied the effect of nitrate ion on critical pitting temperature (CPT) of 2205 duplex stainless (DSS 2205) in 0.6 M NaCl solution by employing potentiodynamic and potentiostatic polarisation experiments. Afterward, a mechanistic approach was arranged based on CPT model proposed by Newman. To this purpose, the effect of nitrate ion on limiting current density in 0.6 M NaCl solution and on the critical current density necessary for passivity in a simulated pit medium (5 M HCl solution) was investigated.

2. Experimental procedure

2.1. Material preparation

A plate of 2205 duplex stainless steel in 50 mm thickness with a chemical composition listed in Table 1 was used to study the effect of nitrate ion (NO_3^-) on critical pitting temperature (CPT). A flat sample was prepared for microstructural observation. Grinding was performed using silicon carbide papers of 60–1200 grit size. Specimen was polished by 0.3 μm alumina slurry and then was electro-etched in 4 M KOH solution at 25 °C, at 2 V DC applied potential for about 30 s. For the purpose of CPT measurements, the plate was machined into 40 mm × 10 mm specimens with hemispherical end to avoid crevice corrosion in pitting experiments. Before immersion, rod specimens were wet ground from 60 to 1200 grit, washed with deionized water and dried with warm air. A copper wire was used to make connection with specimens through non-hemispherical end by using a screw. Immersed surface area was ca. 5 cm^2. In order to avoid of miscalculating in exposed area due to steam presence in the sealed cell, a tape was stuck on that part of sample that was not exposed to the solution. After each test, the specimen checked out carefully with a magnifier to ensure the absence of any water line pitting. All the specimens were solution annealed at 1050 °C for 45 min and then water quenched.

To manufacture pencil electrodes, a thin plate of DSS 2205 alloy was cut into wires with 0.5 mm diameter by using wire cut. The obtained wires were drawn to produce wires in 0.25 mm diameter. These wires were solution annealed at 1050 °C for 30 min followed by water quenching. Then the wires diameter decreased to 0.2 mm and 0.08 mm by electro-polishing in 70 vol% phosphoric acid at 2 V. Each pencil electrode was prepared finally by soldering a piece of copper wire and mounting in a 10 mm dia. bent tube.

Table 1
Chemical composition of alloy DSS 2205 (wt.%).

Element	C	Ni	Si	Mn	Cr	Mo	N	V	W	Fe
wt.%	0.023	5.31	0.5	1.18	21.61	3.07	0.15	0.136	0.064	Bal.

2.2. Electrochemical evaluation

Gill AC potentiostat (ACM Instruments) and conventional three electrode cell were used. Saturated calomel electrode (SCE) and a platinum foil with 2 cm^2 surface area was used as reference electrode and auxiliary electrode, respectively.

2.2.1. CPT measurements

To investigate the effect of nitrate ion on CPT of DSS 2205, a series of experiments were conducted in 0.6 M NaCl solution in absence and presence of 0.01 M and 0.1 M nitrate ion, which were added as $NaNO_3$. At various temperatures, the specimens were hold at their open circuit potential for 30 min and then potentiodynamically polarised from 50 mV cathodic potential respect to OCP until anodic current density reached to 300 μA cm^{-2} owing to ensure that breakdown in passivity (transpassivity or pitting) was occurred. The sweep rate of potentiodynamic tests was 30 mV min^{-1}. The potential at which the current density exceeded from 100 μm cm^{-2} and continues to rise was considered as the breakdown potential [19,23]. The criterion for alloy CPT was the temperature at which the breakdown potential drops steeply. Potentiostatic polarisation tests were carried out at anodic applied potential of 650 mV (SCE) and temperature was increased at a rate less than 0.6 °C min^{-1} until the current density reached to 300 μA cm^{-2}. The temperature at which current density exceeded to 100 μA cm^{-2}, was considered as the alloy CPT [19,23]. Prepared solutions for these experiments were deaerated with almost pure nitrogen for 30 min before and during the tests. Each test was repeated for at least three times to ensure reproducibility.

2.2.2. Pencil electrode studies

Critical current density of 200 μm dia. DSS 2205 pencil electrode was assessed in simulated pit electrolyte at various temperatures. The effect of nitrate ion addition on i_{crit} was studied by adding 0.1 M $NaNO_3$ into 5 M HCl solution. The samples were ground up to 1200 grit and then were put face up in the solution. Open circuit potential was measured for 30 min and then potentiodynamic polarisation was conducted from 50 mV cathodic potential up to 2000 mV anodic potential respect to rest potential at a scan rate of 300 mV min^{-1}.

The effect of nitrate ion on limiting current density was investigated by using 80 μm dia. pencil electrode in 0.6 M NaCl solution in absence and presence of 0.02 M NO_3^- added as $NaNO_3$. The specimens were ground with 60 emery paper to create preferential sites for pit initiation. The specimens were placed upward in the solution. The applied anodic potential was 850 mV (SCE) to ensure that stable pitting occurs and an artificial pit could be produced by coalescence of smaller stable pits. After 3750 s, the potential was reversed at a scan rate of 60 mV min^{-1} until specimen is repassivated. Current density was recorded during the test and pit depth was calculated by applying Faraday's second law (Eq. (2)) and assuming stoichiometric dissolution of Fe, Cr and Ni ($n = 2.23$), a mean atomic weight of $Z = 55.2$ g mol^{-1}, density of $\rho = 7.87$ g cm^{-3} and Faraday's constant of $F = 96{,}500$ C mol^{-1}.

$$\delta = \frac{z}{nF\rho}\int i\mathrm{d}t \tag{2}$$

According to Peguet et al. [50], in a very small surface area, the transition from transpassivity to pitting occurs in a transition temperature interval (TTI) instead of an exact CPT. Thus, it seems reasonable that in the case of pencil electrode, pitting corrosion does not occur in the temperature similar to which observed for large specimen. Therefore, to increase the reproducibility, the solutions were hold at 85 °C to make the attainment of single pit possible and then test solution was cooled down to 65 °C. Each test repeated for 5 times to ensure reliability.

3. Experimental results

3.1. Microstructure observation

Fig. 1(a and b) displays different magnifications of the solution annealed DSS 2205 microstructure along the transverse direction. The microstructure shows austenite islands (light regions) embedded in the continuous ferrite matrix (darker phase). Quantitative metallography using MIP™ software, confirmed almost equal phase volume fraction of two phases (49 ± 1 vol% ferrite) in the microstructure.

3.2. CPT measurement

3.2.1. Potentiodynamic polarisation

Fig. 2a illustrates the anodic polarisation curves of 2205 duplex stainless steel in 0.6 M NaCl at different temperatures. As observed, the breakdown potential (E_b) decreases with increase in temperature and drops from ca. 1100 mV (SCE) at 25 °C to ca. 108 mV (SCE) at 85 °C. The passivity breakdown of alloy at temperatures

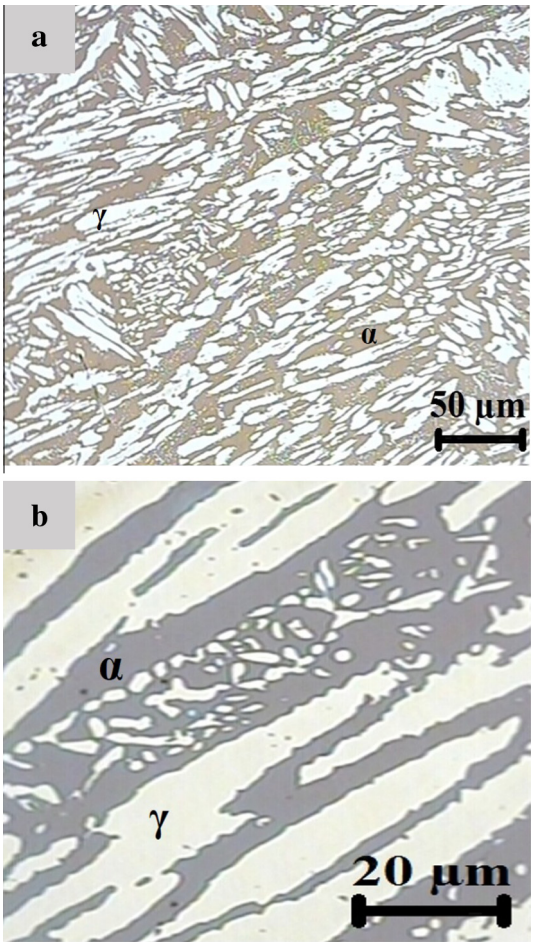

Fig. 1. The microstructure of solution annealed DSS 2205 in different magnifications representing ferrite (dark region) and austenite (brighter region) phases.

of 25–45 °C is due to transpassivity, while a drastic drop in breakdown potential (to 606 mV (SCE)) takes place at temperature of 55 °C indicating the transition of transpassivity to pitting corrosion at this temperature. Further increase in temperature leads to further decrease in breakdown potential. It should be noted that cyclic polarisation confirmed the pitting corrosion at 55 °C. Fig. 2b shows the current density vs. potential curves at various temperatures in sodium chloride solution after addition of 0.01 M nitrate. Comparing the results shown in Fig. 2b and the results obtained from polarisation in absence of nitrate ions revealed that addition of 0.01 M NO_3^-, apart from the increase in E_b, has no effect on pitting behaviour of DSS 2205. Further studies revealed that 0.1 M NO_3^- has a great inhibition effect in pitting corrosion. As it is apparent in Fig. 2c, in presence of 0.1 M nitrate ion, pitting corrosion does not occur even at the temperature of 85 °C. In addition, some fluctuations of current density are observable in passivity region before sharp increase of current density in all solutions (Fig. 2). In the absence and presence of 0.01 M nitrate ion, fluctuations with very high amplitude are observable at temperatures above 45 °C, while by increasing nitrate ion to 0.1 M, these fluctuations have less frequency and are observed at temperatures higher than 65 °C.

Fig. 3 summarises the breakdown potentials as a function of test temperature. As it can be seen, the presence of 0.01 M nitrate ion slightly increases the breakdown potential. Although, similar to what occurs in 0.6 M NaCl solution, the value of E_b decreased dramatically at 55 °C. It could be concluded that critical pitting temperature of alloy in 0.6 M NaCl solution is a temperature between 45 °C and 55 °C. This also can be found that 0.01 M nitrate is not high enough to increase alloy CPT. It is evident that there is a significant increase in breakdown potential value in 0.6 M NaCl + 0.1 M $NaNO_3$ solution. No abrupt drop in breakdown potential occurs at temperatures up to 85 °C. In other words, addition of 0.1 M nitrate raises CPT more than of 30 °C and shifts it to temperatures higher than 85 °C. According to potentiodynamic results, the lowest concentration of nitrate ion required for improving pitting corrosion resistance and affecting the CPT of DSS 2205 in 0.6 M NaCl is a value between 0.01 M and 0.1 M.

For the purpose of comparison, potentiodynamic curves of alloy in 1 M NaCl with 0, 0.01, and 0.1 M nitrate ion at 85 °C are shown in Fig. 4. It could be seen that increase in nitrate concentration makes no sensible change in E_{corr} and slightly decreases the passive current density. In addition, a noticeable increase in breakdown potential is apparent in the presence of 0.1 M NO_3^-. Noteworthy among is the potential at which the abrupt increase in current density occurs in the absence of nitrate ion. In a slightly higher potential, this increment in current density occurs in presence of 0.01 M nitrate. Even after addition of 0.1 M NO_3^-, the sudden increase in current density is observable in this potential, but presence of nitrate leads to repassivation of pit. Subsequently, current density falls to the passivity range and remains steady until potential reaches to transpassivity region. At 65 °C and 75 °C, the same behaviour is observed.

3.2.2. Potentiostatic CPT measurements

Fig. 5 illustrates the results of CPT assessments at different nitrate ion concentrations. Considering the temperature related to 0.1 mA cm^{-2} current density as alloy CPT, the critical pitting temperature of DSS 2205 in 0.6 M NaCl is 53 °C. In the presence

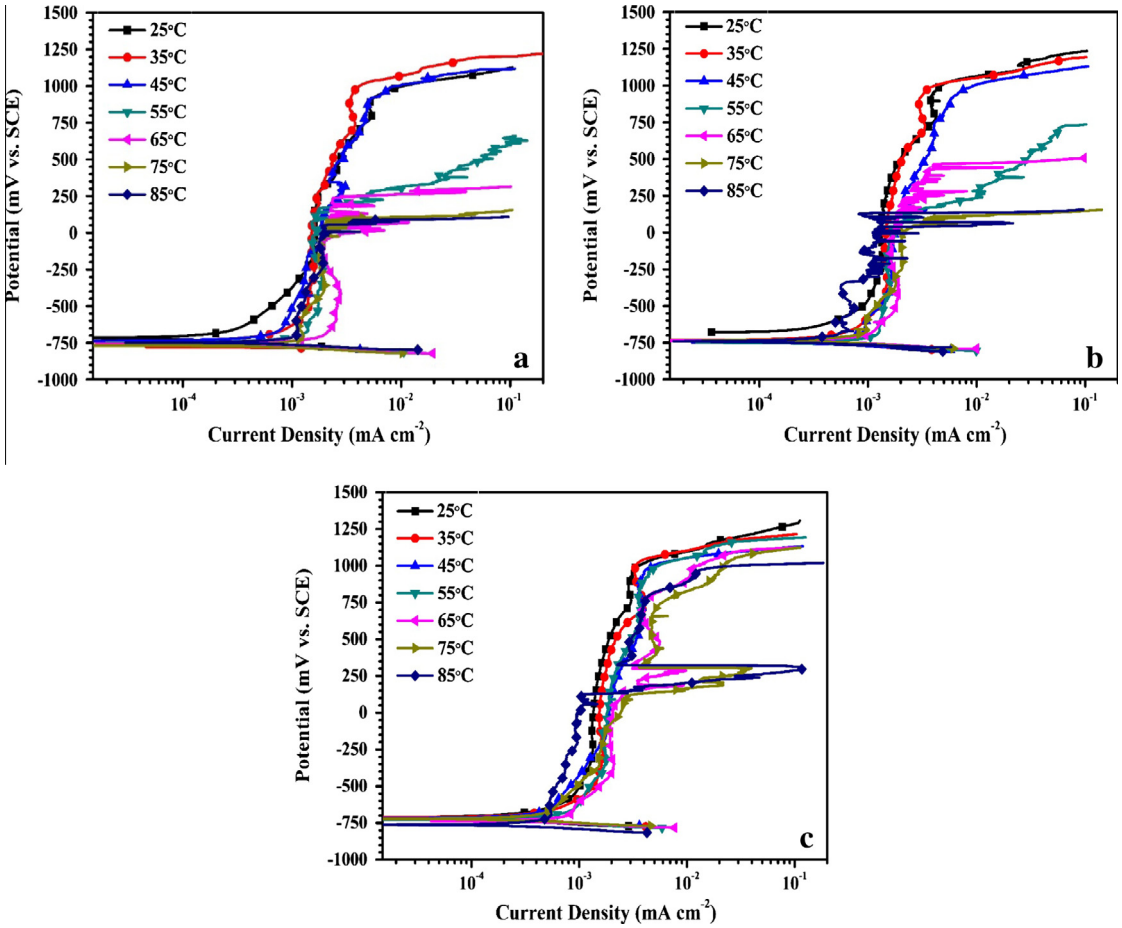

Fig. 2. Potentiodynamic curves for DSS 2205 at different temperatures in (a) 0.6 M NaCl, (b) 0.6 M NaCl + 0.01 M $NaNO_3$, (c) 0.6 M NaCl + 0.1 M $NaNO_3$. The sweep rate was 0.5 mV s^{-1}.

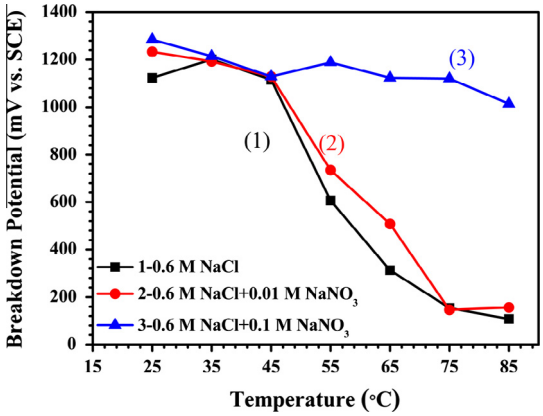

Fig. 3. Breakdown potentials correspond to 0.1 mA cm^{-2} for DSS 2205 obtained from potentiodynamic polarisation conducted at different temperatures. The sweep rate was 0.5 mV s^{-1}.

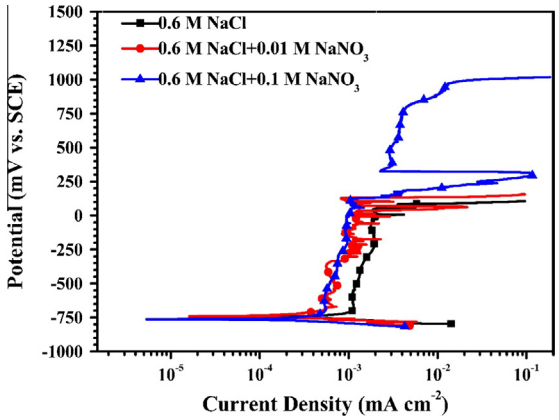

Fig. 4. Potentiodynamic curves for DSS 2205 in chloride solution with various concentration of nitrate, at 85 °C. The sweep rate was 0.5 mV s^{-1}.

of 0.01 M nitrate ion (0.6 M NaCl + 0.01 M $NaNO_3$) only almost 2 °C increase in CPT is observable. After addition of 0.1 M nitrate to the chloride containing solution (0.6 M NaCl + 0.1 M $NaNO_3$), obtained current density is in the range of passivity and no abrupt increase is observed up to 85 °C (upper limit of water bath temperature). Therefore, it could be concluded that 0.1 M NO_3^- is sufficient for increasing CPT to temperatures above 85 °C.

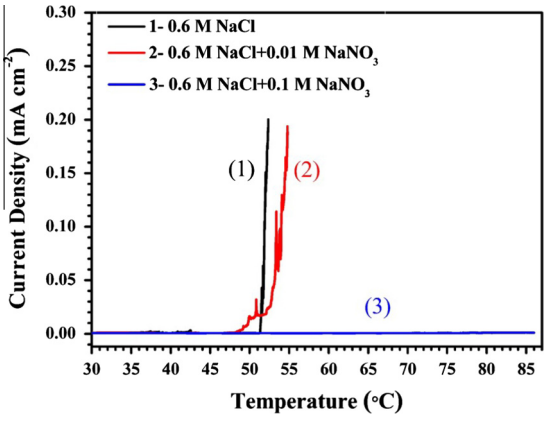

Fig. 5. Potentiostatic current–temperature for CPT evaluation of 2205 DSS at applied anodic potential of 650 mV (SCE). Temperature increasing rate was 0.3 °C min^{-1}.

3.3. Pencil electrode studies

3.3.1. Assessment of critical current density (i_{crit})

Obtained results from potentiodynamic polarisation conducted on 2205 DSS in 5 M HCl solution in absence and presence of 0.1 M NO_3^- have been illustrated in Fig. 6a and b, respectively. Depicted figures show that similar to happen in 0.6 M NaCl solution, addition of nitrate ion to 5 M HCl solution had no effect on E_{Corr}. As observed, the overall behaviour of polarisation curves in both solutions is analogous and after an increase in current density, it was encountered with a dramatic decrease in both solutions. This inflection point defined as the critical current density necessary for passivity (i_{crit}). it is perceived that at temperatures less than 55 °C, the critical current density related to DSS 2205 in acid solution free of nitrate ions, had more values in compare with nitrate containing solution but this behaviour was inverted at 65 °C. Furthermore, for 2205 DSS in free nitrate solution, a sharp increment in current density is observable at high potentials at temperatures up to 45 °C. This behaviour changed at 55 °C and plateau region occurred at higher current density values in compare with temperatures less than 55 °C and continued without any sharp increase. Nevertheless, for nitrate containing nitrate acidic solution, this behavioural change occurred at 65 °C. Furthermore, many fluctuations in current density are observable in plateau region at temperatures above 45 °C in pure hydrochloride and above 55 °C in nitrate containing solution. Additionally, for 2205 DSS in the 0.6 M NaCl + 0.1 M $NaNO_3$ solution, it is observed that current density during reduction stage, is stabilised for a while and then decreased to the values that less temperatures reached after their current density reduction and then similar to them, at higher potentials, the current density increases continuously.

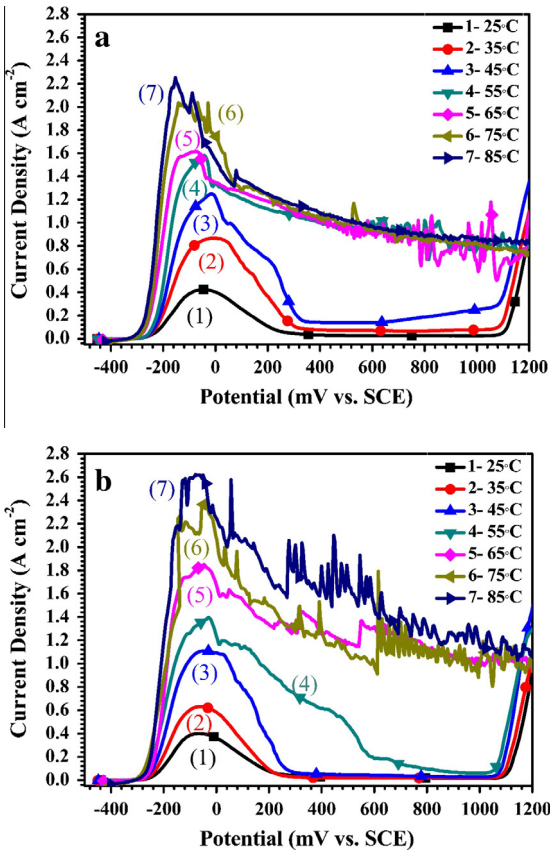

Fig. 6. Current density–potential curves for 200 μm dia. DSS 2205 pencil electrode obtained from potentiodynamic polarisation in (a) 5 M HCl, (b) 5 M HCl + 0.1 M $NaNO_3$ solutions at different temperatures. The sweep rate was 5 mV s^{-1}.

The median values of critical current densities obtained from potentiodynamic polarisation are plotted against temperature in Fig. 7. It is obvious that the critical current density values are augmented with increasing in temperature in both nitrate and free nitrate containing solutions. In HCl solution, the slope of increasing trend changes at 55 °C. Whereas, in presence of 0.1 M NO_3^-, critical current density increases linearly with increasing temperature up to 85 °C. The best trend lines were fitted to the mean values of i_{crit} in each medium (see Fig. 7). To approximate the actual values of i_{crit} at temperatures above the temperature that change in upward trend occurs, the linear part of increasing trend was extrapolated to higher temperatures. It is clear that presence of 0.1 M nitrate ion leads to decrease in critical current density of DSS 2205 and reduces the slope of changing trend slightly in comparison with nitrate free solution.

3.3.2. Assessment of limiting current density (i_{lim})

In order to identify the effect of nitrate ion on pit solution, polarisation of 80 μm DSS 2205 pencil electrodes at 850 mV (SCE) was performed at 85 °C.

Experiments were first conducted in 0.6 M NaCl and 0.6 M NaCl + 0.1 M $NaNO_3$. It is notable that the test conducted in presence of 0.1 M NO_3^- ion, were not reproducible. Based on the view that addition of 0.01 M nitrate has negligible effect on CPT of DSS 2205 (as discussed in Sections 3.2 and 3.3), therefore further experiments were necessary to detect the appropriate nitrate concentration beneficial for the CPT of DSS 2205. Therefore, potentiodynamic polarisation tests were performed at temperatures above 55 °C in presence of various concentrations of nitrate ions (between 0.01 M and 0.1 M).

Potentiodynamic results illustrated in Fig. 8 is obtained in presence of 0.02 M NO_3^- implying that in presence of 0.02 M nitrate ion, the alloy CPT lies between 55 °C and 65 °C which shows 10 °C increase in comparison with CPT obtained in 0.6 M NaCl solution (see Fig. 2a in Section 3.2). Therefore, other concentrations of nitrate ion were not examined and 0.6 M NaCl + 0.02 M NO_3^- was selected as experimental solution for the purpose of comparison to pure sodium chloride medium and evaluation of nitrate addition on pit solution chemistry and limiting current density.

A typical current density vs. time curve obtained from potentiostatic test conducted in 0.6 M NaCl and 0.6 M NaCl + 0.02 M $NaNO_3$ solutions is displayed in Fig. 9. As it is depicted in this figure, the plateau region observed in the curve related to nitrate containing solution is located in higher current densities in compare with free nitrate solution. *i–t* curve obtained from potentiodynamic test (reverse scan) is illustrated in Fig. 10 to make a better understanding of current density variation through the tests employed in this stage. The information that could be extracted from this curve, was shown completely in literature [44].

Fig. 11 displays a typical square of current density (i^2) vs. time curves (obtained from data in plateau region of *i–t* curves shown in Fig. 9). Combination of (Eq. (1)) and Faraday's second law (Eq. (2)) yields Eq. (3) which indicates that in diffusion-controlled region, i^2 changes with reverse of time.

$$i^2 = \frac{n^2F^2\rho DC_S}{Z} \times t^{-1} \quad (3)$$

The linear relation between i^2 and t^{-1} confirms that the dissolution of cations into the pit is under diffusion control in this region. Furthermore, it is apparent in Fig. 11 that addition of 0.02 M nitrate ion leads to increase in the curvature slope.

Additionally, by comparing current density vs. pit depth, calculated using Faraday's second law (Eq. (2)), curves in the region which current density is under diffusion control (illustrated in Fig. 12), it is obvious that in a same pit depth, the current density in diffusion limiting stage (i_{lim}) is noticeably higher in presence of nitrate ion. Indeed, the mean values of i_{lim} are increased from 144 mA cm^{-2} in 0.6 M NaCl to 224 mA cm^{-2} in 0.6 M NaCl + 0.02 M $NaNO_3$.

Fig. 13 shows the calculated values of $D.C_S$ obtained from *i–t* curve for DSS 2205 pencil electrode in both test solutions vs. pit depth indicating that $D.C_S$ is increased in presence of 0.02 M nitrate ion. By considering the constant value of 10^{-5} cm^2 s^{-1} for *D*, it could be concluded that the mean value of C_S (concentration of cations necessary for metal salt precipitation) increased from 3.40×10^{-3} mol cm^{-3} in chloride solution to 7.10×10^{-3} mol cm^{-3} in 0.02 M nitrate containing solution.

4. Discussion

4.1. Potentiodynamic polarisation

Based on the increase in passivity current density and because of the breakdown potential (E_b) decrement with temperature increasing, it can be concluded that in absence and presence of nitrate ion, the resistance of DSS 2205 to pitting corrosion decreases with temperature. According to Wang et al. [51], the amount of defects existed in the passive layer as well as the

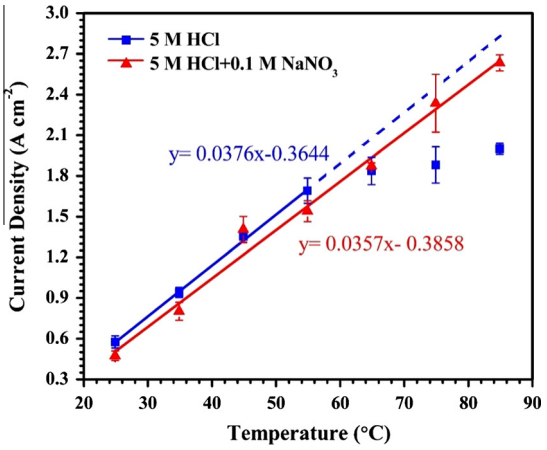

Fig. 7. Mean values of critical current density for 200 μm dia. DSS 2205 pencil electrode obtained from potentiodynamic polarisation in simulated pit solution in absence and presence of 0.1 M $NaNO_3$ at different temperatures alongside of best fitted trend lines fitted to mean values of critical current density. The sweep rate was 5 mV s^{-1}. Error bars represent 95% confidence limits measured from at least five experimental tests under identical conditions.

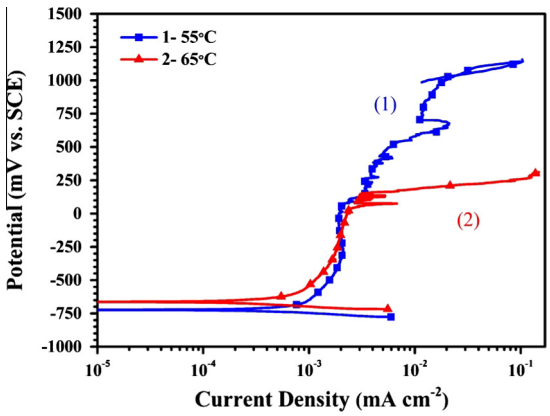

Fig. 8. Potentiodynamic curves for DSS 2205 in 0.6 M NaCl + 0.02 M $NaNO_3$ at different temperatures. The sweep rate was 0.5 mV s^{-1}.

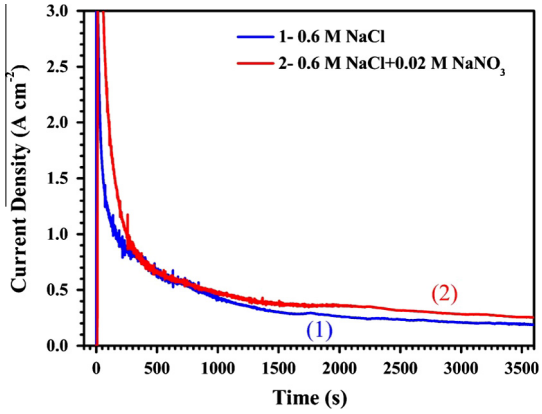

Fig. 9. Current density vs. time curves for 80 μm dia. DSS 2205 pencil electrode obtained from potentiostatic polarisation conducted at applied anodic potential of 850 mV (SCE) in 0.6 M NaCl and 0.6 M NaCl + 0.02 M $NaNO_3$ solutions at 65 °C.

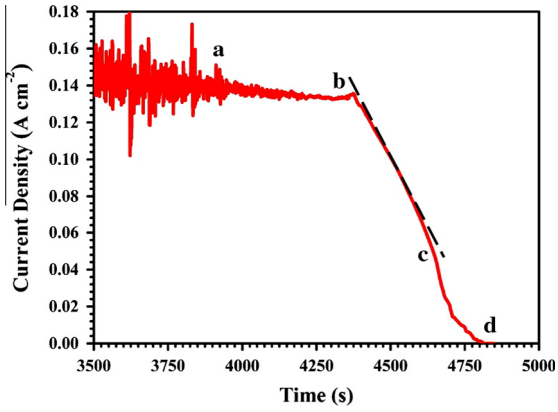

Fig. 10. Current density vs. time curves for 80 μm dia. DSS 2205 pencil electrode obtained from potentiodynamic polarisation conducted after potentiostatic test from anodic potential of 850 mV (SCE) to corrosion potential in 0.6 M NaCl and 0.6 M NaCl + 0.02 M $NaNO_3$ solutions at 65 °C. The sweep rate was 1 mV s^{-1}. The potentiodynamic test was started after 3750 s, but to make a better understanding of current density behaviour, this figure is illustrated from final seconds of potentiostatic test.

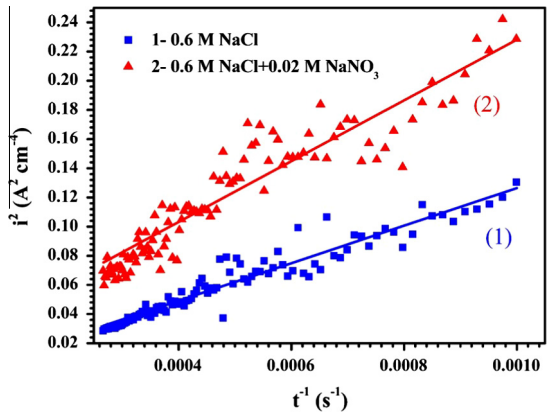

Fig. 11. i^2 vs. t^{-1} curves for 80 μm dia. DSS 2205 pencil electrode obtained from *i–t* curve at 65 °C.

amount of oxide film vacancies increase at high temperatures owing to Cl^- ion attendance in passive layer formed on metal surface and due to the fundamental alteration occurs in chemical composition or physical arrangement of passive layer, respectively.

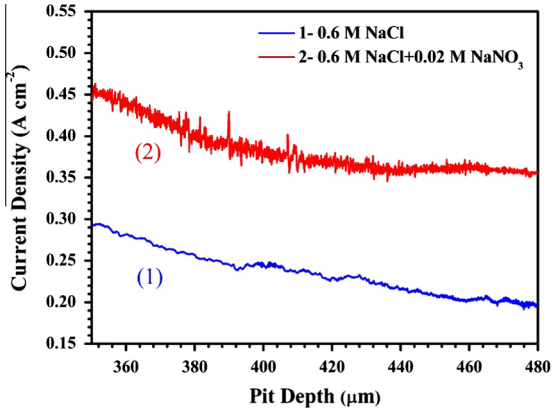

Fig. 12. Current density vs. pit depth curves for 80 μm dia. DSS 2205 pencil electrode calculated from *i–t* curve at 850 mV (SCE) at 65 °C, pit depths are calculated using Faraday's second law.

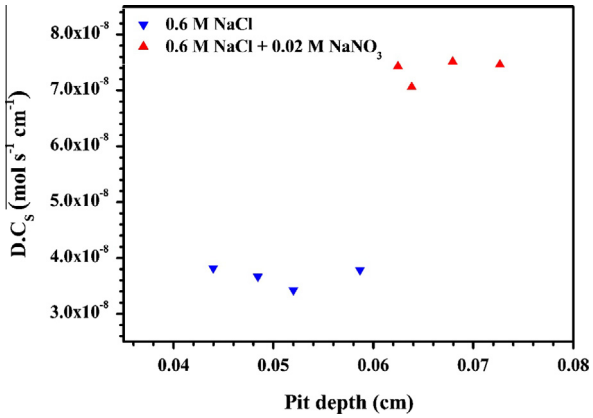

Fig. 13. $D.C_S$ as a function of pit depth for 80 μm dia. DSS 2205 pencil electrode obtained from *i–t* curves at 65 °C.

Consequently, the breakdown potential shifts down with increasing temperature in all solutions.

According to Newman and Ajjawi [33], nitrate ion does not affect the active dissolution and only influence on salt covered surfaces. Sudden increase of current density at temperatures above 65 °C at approximately same potential which pitting occurs in other test solutions (Figs. 2c and 3), indicates that in presence of 0.1 M nitrate ion, initiation and growth of pit occurs and subsequent repassivation of pit in presence of nitrate ion results in an steep fall to passivity domain.

To explain the ineffectiveness of nitrate ion on E_{corr}, the cathodic and anodic reactions should be considered. Based on thermodynamic requirements consideration as well as chemical composition of solution and its pH, the below electrochemical reactions are introduced as possible anodic reactions [52]:

$$Fe + 2H_2O = Fe(OH)_2 + 2H^+ + 2e^- \quad E_{eq} = -0.10 - 0.059pH \tag{4}$$

$$Cr + 3H_2O = Cr(OH)_3 + 3H^+ + 3e^- \quad E_{eq} = -0.579 - 0.059pH \tag{5}$$

$$2Fe + 3H_2O = Fe_2O_3 + 6H^+ + 6e^- \quad E_{eq} = -0.059 - 0.059pH \tag{6}$$

$$3Fe + 4H_2O = Fe_3O_4 + 8H^+ + 8e^- \quad E_{eq} = -0.085 - 0.059pH \tag{7}$$

Moreover, cathodic reactions are as below [30,33,34]:

$$O_2 + 2H_2O + 4e^- = 4OH^- \quad E_{eq} = 1.198 - 0.059pH \tag{8}$$

$$NO_3^- + 2H^+ + e^- = NO_2 + H_2O$$
$$E_{eq} = 0.80 - 0.118pH + 0.059\log[NO_3^-] \quad (9)$$

$$NO_3^- + 10H^+ + 8e^- = 3H_2O + NH_4^+$$
$$E_{eq} = 0.40 - 0.074pH + 0.007\log[NO_3^-] \quad (10)$$

$$NO_3^- + 2H^+ + 2e^- = NO_2^- + 3H_2O$$
$$E_{eq} = 1.027 - 0.059pH + 0.0295\log[NO_3^-] \quad (11)$$

where E_{eq} represents equilibrium potential and all potentials refer to standard hydrogen electrode (SHE).

In 0.6 M NaCl solution, only Eq. (8) is considered as cathodic reaction, but in presence of nitrate ion, three other introduced reactions are involved, as well. According to Eqs. (8)–(11), negligible effect of nitrate ion on free corrosion potential seems reasonable. On the other hand, based on the fact that all cathodic reactions stated above are acid consuming reactions, it can be concluded that presence of nitrate ion increases pH of the local solution within the pit and consequently, leads to pit growth inhibition by vanishing the low pH environment necessary for pit growth. In addition, nitrite ion produced as a result of nitrate reduction, is also a possible reason of inhibiting effect of nitrate. According to Reffass et al. [25], the passive layer formed on metal surface is composed of Iron (III) species; therefore, the inhibitive effect of nitrite ion might be associated with its effect on oxidisation of Iron (II) into Iron (III). One another reason is based on competitive absorption between nitrate and Cl^- ions. Nitrate ion probably affects the absorption of chloride ions and adsorb on the passive layer itself and consequently leads to the improvement of passive layer self-healing [49].

4.2. Potentiostatic polarisation

Current density fluctuations observed in passive region of potentiostatic results of DSS 2205 in both free nitrate and 0.01 M nitrate-containing solutions (Fig. 5) are associated with formation and repassivation of metastable pits.

The fluctuations observed during pit growth and the gradual current density increasing observed in 0.01 M nitrate-containing solution could be due to presence of insufficient nitrate ion concentration. Although the presence of nitrate ion leads to local passivity to occur on the metal surface, but since 0.01 M NO_3^- is not enough to produce complete passivity, the local passive layer is wiped out and consequently, pit growth continues on metal surface. The accelerated pit initiation observed in presence of 0.01 M nitrate ion followed by retarded growth, is in accordance with the literature reported by Chou et al. [30].

4.3. Pencil electrode study

4.3.1. Critical current density (i_{crit})

The reduction in current density occurred immediately after achieving the current density to the maximum value, could be due to either passivity of metal surface or salt film precipitation on alloy surface. In the polarisation curves at which current density increment occurs due to transpassivity, sudden current density drop occurs as a result of surface passivity when current density reaches to the maximum value. On the other side, reduction in current density occurs as a result of salt precipitation, leads the current density to remain in an approximately constant value representing diffusion limiting current density. Small plateau region followed by passivity region observed in presence of 0.1 M NO_3^- at 55 °C, could be indicative of diffusion controlled current density due to salt precipitation and passivity under the salt covered surface. This observation is completely consistent to what reported by Newman and Shahrabi [34] about passivation of austenitic stainless steel in 4 M HCl + 0.3 M $NaNO_3$. This could be explained according to what suggested about the necessarily of presence of metal salt on nitrate effectiveness [33]. In other words, since the arisen pit encountered passivity and consequently, the current density decreases to passivity region, it could be concluded that salt precipitation, alongside of sufficient nitrate concentration, leads nitrate ion to be effective and decrease current density to the passive region. Possible reason for the observation of fluctuations in current density in diffusion controlled stage in both test solutions, might be local passivation and reactivation under precipitated salt film [33].

The decline observed in the slope of current density vs. temperature curve of nitrate containing solution in comparison with nitrate free solution, indicates that the presence of NO_3^- leads to decrease in the value of critical current density in comparison with pure acidic solution. This could be due to reaction in which acid is consumed by nitrate ion and water is produced (Eqs. (8)–(11)). Based on CPT definition (i.e. the temperature at which $i_{lim} = i_{crit}$) [43] and regardless of the effect of nitrate ion on i_{lim}, it can be concluded that presence of sufficient nitrate ion leads to increase in the CPT of DSS 2205.

4.3.2. Limiting current density (i_{lim})

The sharp rise in current density observed in Fig. 10 is due to unifying of small formed stable pits on pencil electrode surface under the applied potential. Once the single pit created as a result of pits coalescence, the current density reached to its maximum value. During pit growth, alloying elements (Fe, Cr and Ni) are dissolved under activation control and entered to the pit in the form of their cations [53]. After formation of single artificial pit and salt precipitation, the current density starts to decrease until the establishment of salt diffusion controlled dissolution and subsequently reaches to the almost steady state. This condition continues even after reverse scanning of the potential while the metal salt exists at the pit bottom (Fig. 10). This is because of the fact that diffusion controlled current density is independent of salt film thickness [35]. Considering what Laycock and Newman [54] suggested about the three different resistance sources existed between the reference electrode and metal surface, it can be conclude that decreasing the potential leads to reduction in the salt layer resistance and since the salt layer thickness controls its resistance [36], therefore the salt layer thickness reduced. Due to Isaacs and Newman [37], further decrease in potential provides favourable condition for passivity occurrence in consequence of decreasing the concentration of dissolved cations. The current density at which the salt layer vanishes completely, is defined as limiting current density (i_{lim}) and correlated cation concentration required for salt precipitation defines as saturation concentration (C_S) (Fig. 10, point b). Afterward, obeying Ohm's law and under ohmic activation control, the current density continues to decrease. By further lowering the potential, cation concentration reaches to critical concentration (C^*) essential for a pit to be stable (Fig. 10, point c) and in concentrations less than C^*, the pit becomes passive (Fig. 10, point d).

Similar to the results that Newman and Ajjawi have reported for 304 stainless steel [33], fluctuations observed in current density vs. time curves (Figs. 9 and 10) and current density vs. pit depth curves (Fig. 12) of both test solutions are real and could be due to occurrence of local passivity and surface reactivation under the salt layer.

By assuming the identical value of n, F, ρ, and Z in Eq. (3), the slope of i^2 against reciprocal of time can be applied for estimation of $D.C_S$. Therefore, increased slope of i^2 vs. t^{-1} in the presence of nitrate ions (Fig. 11) could imply that saturation concentration of metal cations in pit solution increases in the presence of nitrate ion. Change in variation of pit depth vs. time in the presence of

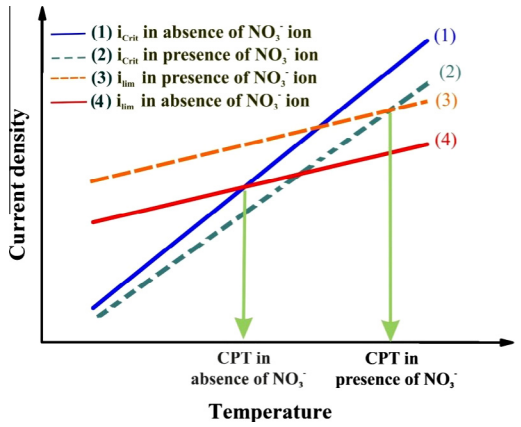

Fig. 14. Schematic diagram to show how nitrate ion effects the critical pitting temperature (CPT) of DSS 2205 due to change in i_{lim} and i_{crit} based on theory proposed by Salinas Bravo and Newman who introduced CPT as a temperature at which $i_{lim} = i_{crit}$.

nitrate ion (depicted in Fig. 12). Since the mobility number of NO_3^- is close to Cl^- mobility number [31], it is able to enter the pit alongside the Cl^- to neutralise the produced electric charge within the pit. As a result of nitrate ion entrance into pit solution, the composition of salt precipitated at the pit bottom can probably change from $FeCl_2$ for 0.6 M NaCl solution to the $FeCl_2 + Fe(NO_3)_2$ for nitrate containing solution. Therefore, due to change in chemical composition of precipitated metal salt at the pit bottom in presence of nitrate ion, the value of minimum concentration of metal cations needed for salt precipitation (C_S) increases and subsequently, based on Eq. (1), the value of limiting current density (i_{lim}) increases. Frankly, since the pit depth has been increased in presence of nitrate ion (Fig. 13), it is expected that the amount of i_{lim} decrease in presence of nitrate ion (based on Eq. (1)). However, $D.C_S$ value increases to a value not only enough to compensate for the decrease in current density, but also leads to increase in the value of i_{lim} (Figs. 9 and 12). In other words, temperature should be increased to provide the essential concentration for salt precipitating at the pit bottom. Based on the CPT definition proposed by Salinas Bravo and Newman (i.e. the temperature at which $i_{lim} = i_{crit}$) [43], by increasing the value of limiting current density, the CPT of DSS 2205 increases (Fig. 14). However, in the purpose of verifying this suggestion, further studies are necessary to ensure about the composition of precipitated salt layer in presence of nitrate ion.

The outcome of what mentioned above is schematically depicted in Fig. 14 to show how nitrate ion presence improves CPT by affecting on the amounts of i_{lim} and i_{crit}.

5. Conclusion

In this research, the effect of nitrate ion on critical pitting temperature (CPT) of 2205 duplex stainless steel (DSS 2205) was investigated in NaCl medium employing electrochemical and mechanistic approaches. The results could be summarised as below:

1. Potentiodynamic polarisation show that addition of 0.01 M nitrate ion has no effect on CPT of DSS 2205, although increases breakdown potential (E_b) in comparison with 0.6 M NaCl solution. By increasing nitrate to 0.1 M, the pitting corrosion was not occurred up to 85 °C.
2. Potentiostatic test revealed that in the presence of 0.01 M nitrate ion, the CPT increases approximately 2 °C and similar to obtained results from potentiodynamic test, the pitting corrosion was not observed up to 85 °C in presence of 0.1 M nitrate. A noticeable behaviour in presence of 0.01 M nitrate ion was observed. In this nitrate concentration, although the pit initiation is accelerated in compare with free nitrate ion solution, but the pit growth retarded.
3. The tests performed in simulated pit solution (5 M HCl) in absence and presence of 0.1 M nitrate ion using 200 μm dia. pencil electrode, revealed that nitrate ion presence slightly decreased the critical current density essential for passivity (i_{crit}).
4. The tests performed in 0.6 M NaCl solution in absence and presence of 0.02 M nitrate ion using 80 μm dia. pencil electrode, show that nitrate presence leads to increase in $D.C_S$ and limiting current density (i_{lim}).
5. Based on CPT definition proposed by Newman and Ajjawi, it can be concluded that by increasing i_{lim} and decreasing i_{crit} in presence of nitrate ion, the intersection of these two variations shifts to higher temperature and consequently, the CPT of DSS 2205 increases.

Acknowledgment

Authors would like to appreciate financial support from Ferdowsi University of Mashhad (FUM) for providing the laboratory facilities during period that this research was conducted.

References

[1] V.S. Moura, L.D. Lima, J.M. Pardal, A.Y. Kina, R.R.A. Corte, S.S.M. Tavares, Influence of microstructure on the corrosion resistance of the duplex stainless steel UNS S31803, Mater. Charact. 59 (2008) 1127–1132.
[2] A.M. do Nascimento, M.C.F. Ierardi, A.Y. Kina, S.S.M. Tavares, Pitting corrosion resistance of cast duplex stainless steels in 3.5%NaCl solution, Mater. Charact. 59 (2008) 1736–1740.
[3] G.S. Frankel, Pitting corrosion of metals: a review of the critical factors, J. Electrochem. Soc. 145 (1998) 2186–2198.
[4] P.C. Pistorius, G.T. Burstein, Metastable pitting corrosion of stainless steel and the transition to stability, Philos. Trans. R. Soc. London, Ser. A 341 (1992) 531–559.
[5] R.J. Brigham, E.W. Tozer, Temperature as a pitting criterion, Corrosion 29 (1973) 33–36.
[6] R.J. Brigham, E.W. Tozer, Effect of alloying additions on the pitting resistance of 18% Cr austenitic stainless steel, Corrosion 30 (1974) 161–166.
[7] H. Tan, Y. Jiang, B. Deng, T. Sun, J. Xu, J. Li, Effect of annealing temperature on the pitting corrosion resistance of super duplex stainless steel UNS S32750, Mater. Charact. 60 (2009) 1049–1054.
[8] L. Chen, H. Tan, Z. Wang, J. Li, Y. Jiang, Influence of cooling rate on microstructure evolution and pitting corrosion resistance in the simulated heat-affected zone of 2304 duplex stainless steels, Corros. Sci. 58 (2012) 168–174.
[9] B. Deng, Z. Wang, Y. Jiang, H. Wang, J. Gao, J. Li, Evaluation of localized corrosion in duplex stainless steel aged at 850 °C with critical pitting temperature measurement, Electrochim. Acta 54 (2009) 2790–2794.
[10] Z. Zhang, Z. Wang, Y. Jiang, H. Tan, D. Han, Y. Guo, J. Li, Effect of post-weld heat treatment on microstructure evolution and pitting corrosion behavior of UNS S31803 duplex stainless steel welds, Corros. Sci. 62 (2012) 42–50.
[11] M.H. Moayed, N.J. Laycock, R.C. Newman, Dependence of the critical pitting temperature on surface roughness, Corros. Sci. 45 (2003) 1203–1216.
[12] A. Pardo, M.C. Merino, A.E. Coy, F. Viejo, R. Arrabal, E. Matykina, Pitting corrosion behaviour of austenitic stainless steels – combining effects of Mn and Mo additions, Corros. Sci. 50 (2008) 1796–1806.
[13] R.f.a. Jargelius-Pettersson, Electrochemical investigation of the influence of nitrogen alloying on pitting corrosion of austenitic stainless steels, Corros. Sci. 41 (1999) 1639–1664.
[14] H.-B. Li, Z.-H. Jiang, Y. Yang, Y. Cao, Z.-R. Zhang, Pitting corrosion and crevice corrosion behaviors of high nitrogen austenitic stainless steels, Int. J. Miner. Metall. Mater. 16 (2009) 517–524.
[15] B. Deng, Y. Jiang, J. Liao, Y. Hao, C. Zhong, J. Li, Dependence of critical pitting temperature on the concentration of sulphate ion in chloride-containing solutions, Appl. Surf. Sci. 253 (2007) 7369–7375.
[16] M.H. Moayed, R.C. Newman, Aggressive effects of pitting "inhibitors" on highly alloyed stainless steels, Corros. Sci. 40 (1998) 519–522.
[17] M.H. Moayed, R.C. Newman, Deterioration in critical pitting temperature of 904L stainless steel by addition of sulfate ions, Corros. Sci. 48 (2006) 3513–3530.

[18] C.R. Alentejano, I.V. Aoki, Localized corrosion inhibition of 304 stainless steel in pure water by oxyanions tungstate and molybdate, Electrochim. Acta 49 (2004) 2779–2785.
[19] F. Eghbali, M.H. Moayed, A. Davoodi, N. Ebrahimi, Critical pitting temperature (CPT) assessment of 2205 duplex stainless steel in 0.1 M NaCl at various molybdate concentrations, Corros. Sci. 53 (2011) 513–522.
[20] A. Igual Muñoz, J. García Antón, J.L. Guiñón, V. Pérez Herranz, The effect of chromate in the corrosion behavior of duplex stainless steel in LiBr solutions, Corros. Sci. 48 (2006) 4127–4151.
[21] A. Igual Muñoz, J. García Antón, J.L. Guiñón, V. Pérez Herranz, Inhibition effect of chromate on the passivation and pitting corrosion of a duplex stainless steel in LiBr solutions using electrochemical techniques, Corros. Sci. 49 (2007) 3200–3225.
[22] G.O. Ilevbare, G.T. Burstein, The inhibition of pitting corrosion of stainless steels by chromate and molybdate ions, Corros. Sci. 45 (2003) 1545–1569.
[23] N. Ebrahimi, M.H. Moayed, A. Davoodi, Critical pitting temperature dependence of 2205 duplex stainless steel on dichromate ion concentration in chloride medium, Corros. Sci. 53 (2011) 1278–1287.
[24] M.A. Deyab, S.S. Abd El-Rehim, Inhibitory effect of tungstate, molybdate and nitrite ions on the carbon steel pitting corrosion in alkaline formation water containing Cl^- ion, Electrochim. Acta 53 (2007) 1754–1760.
[25] M. Reffass, R. Sabot, M. Jeannin, C. Berziou, P. Refait, Effects of NO_2^- ions on localised corrosion of steel in $NaHCO_3$ + NaCl electrolytes, Electrochim. Acta 52 (2007) 7599–7606.
[26] M.B. Valcarce, M. Vázquez, Carbon steel passivity examined in alkaline solutions: the effect of chloride and nitrite ions, Electrochim. Acta 53 (2008) 5007–5015.
[27] W. Schwenk, Theory of stainless steel pitting, Corrosion 20 (1964) 129t–137t.
[28] H.H. Uhlig, J.R. Gilman, Pitting of 18-8 stainless steel in ferric chloride inhibited by nitrates, Corrosion 20 (1964) 289t–292t.
[29] H.P. Leckie, H.H. Uhlig, Environmental factors affecting the critical potential for pitting in 18-8 stainless steel, J. Electrochem. Soc. 113 (1966) 1262–1267.
[30] Y.L. Chou, J.W. Yeh, H.C. Shih, Pitting corrosion of $Co_{1.5}CrFeNi_{1.5}Ti_{0.5}Mo_{0.1}$ in chloride containing nitrate solutions, Corrosion 67 (2011). 065003-065001-065003-065007.
[31] Y. Zuo, H. Wang, J. Zhao, J. Xiong, The effects of some anions on metastable pitting of 316L stainless steel, Corros. Sci. 44 (2002) 13–24.
[32] C.S. Brossia, R.G. Kelly, Influence of alloy sulfur content and bulk electrolyte composition on crevice corrosion initiation of austenitic stainless steel, Corrosion 54 (1998) 145–154.
[33] R.C. Newman, M.A.A. Ajjawi, A micro-electrode study of the nitrate effect on pitting of stainless steels, Corros. Sci. 26 (1986) 1057–1063.
[34] R.C. Newman, T. Shahrabi, The effect of alloyed nitrogen or dissolved nitrate ions on the anodic behaviour of austenitic stainless steel in hydrochloric acid, Corros. Sci. 27 (1987) 827–838.
[35] T.R. Beck, R.C. Alkire, Occurrence of salt films during initiation and growth of corrosion pits, J. Electrochem. Soc. 126 (1979) 1662–1666.
[36] H.S. Isaacs, The behavior of resistive layers in the localized corrosion of stainless steel, J. Electrochem. Soc. 120 (1973) 1456–1462.
[37] H.S. Isaacs, R.C. Newman, in: R. P. Frankenthal, F. Mansfeld (Eds.) Corrosion and Corrosion Protection, The Electrochemical Society Proceedings Series, Pennington, NJ, 1981, pp. 120.
[38] G.S. Frankel, L. Stockert, F. Hunkeler, H. Boehni, Metastable pitting of stainless steel, Corrosion 43 (1987) 429–436.
[39] H.S. Isaacs, J.H. Cho, M.L. Rivers, S.R. Sutton, In situ X-ray microprobe study of salt layers during anodic dissolution of stainless steel in chloride solution, J. Electrochem. Soc. 142 (1995) 1111–1118.
[40] H.S. Isaacs, S.M. Huang, Behavior of dissolved molybdenum during localized corrosion of austenitic stainless steel, J. Electrochem. Soc. 143 (1996) L277–L279.
[41] T. Rayment, A.J. Davenport, A.J. Dent, J.-P. Tinnes, R.J.K. Wiltshire, C. Martin, G. Clark, P. Quinn, J.F.W. Mosselmans, Characterisation of salt films on dissolving metal surfaces in artificial corrosion pits via in situ synchrotron X-ray diffraction, Electrochem. Commun. 10 (2008) 855–858.
[42] N. Sridhar, D.S. Dunn, In situ study of salt film stability in simulated pits of nickel by Raman and electrochemical impedance spectroscopies, J. Electrochem. Soc. 144 (1997) 4243–4253.
[43] V.M. Salinas-Bravo, R.C. Newman, An alternative method to determine critical pitting temperature of stainless steels in ferric chloride solution, Corros. Sci. 36 (1994) 67–77.
[44] P. Ernst, R.C. Newman, Pit growth studies in stainless steel foils. II. Effect of temperature, chloride concentration and sulphate addition, Corros. Sci. 44 (2002) 943–954.
[45] P. Ernst, R.C. Newman, Pit growth studies in stainless steel foils. I. Introduction and pit growth kinetics, Corros. Sci. 44 (2002) 927–941.
[46] P.C. Pistorius, G.T. Burstein, Growth of corrosion pits on stainless steel in chloride solution containing dilute sulphate, Corros. Sci. 33 (1992) 1885–1897.
[47] J. Mankowski, Z. Szklarska-Smialowska, Studies on accumulation of chloride ions in pits growing during anodic polarization, Corros. Sci. 15 (1975) 493–501.
[48] T. Suzuki, M. Yamabe, Y. Kitamura, Composition of anolyte within pit anode of austenitic stainless steels in chloride solution, Corrosion 29 (1973) 18–22.
[49] T. Misawa, H. Tanabe, In situ observation of dynamic reacting species at pit precursors of nitrogen-bearing austenitic stainless steels, ISIJ Int. 36 (1996) 787–792.
[50] L. Peguet, A. Gaugain, C. Dussart, B. Malki, B. Baroux, Statistical study of the critical pitting temperature of 22-05 duplex stainless steel, Corros. Sci. 60 (2012) 280–283.
[51] J.H. Wang, C.C. Su, Z. Szklarska-Smialowska, Effects of Cl^- concentration and temperature on pitting of AISI 304 stainless steel, Corrosion 44 (1988) 732–737.
[52] M.G. Fontana, Corrosion Engineering, third ed., Tata McGraw-Hill, 2005.
[53] J.W. Tester, H.S. Isaacs, Diffusional effects in simulated localized corrosion, J. Electrochem. Soc. 122 (1975) 1438–1445.
[54] N.J. Laycock, M.H. Moayed, R.C. Newman, Metastable pitting and the critical pitting temperature, J. Electrochem. Soc. 145 (1998) 2622–2628.